

## Transformation products and mechanistic pathway of levofloxacin degradation in aqueous solution using advanced oxidation processes in the presence of BiVO<sub>4</sub> and visible light

Mohammed A. Meetani<sup>a,\*</sup>, Ahmed Alzamy<sup>a</sup>, Naji Al-Dubaili<sup>a</sup>, Mohamed F. Malik<sup>a</sup>, Nada Elmerhi<sup>a</sup>, Noor I. Albadawi<sup>a</sup>, Soleiman Hisaindee<sup>a</sup>, Rengaraj Selvaraj<sup>b</sup>, Muhammad A. Rauf<sup>a</sup>

<sup>a</sup>Chemistry Department, United Arab Emirates University, Al-Ain, P.O. Box: 15551, UAE, Tel. +971-3-7136136 (Off); Fax: +971-3-7134928; emails: mmeetani@uaeu.ac.ae (M.A. Meetani), ahmed.alzamy@uaeu.ac.ae (A. Alzamy), n.dubaili@uaeu.ac.ae (N. Al-Dubaili), 201350131@uaeu.ac.ae (M.F. Malik), 201350211@uaeu.ac.ae (N. Elmerhi), 201350347@uaeu.ac.ae (N.I. Albadawi), soleiman.hisaindee@uaeu.ac.ae (S. Hisaindee), raufmapk@yahoo.com (M.A. Rauf)

<sup>b</sup>Chemistry Department, Sultan Qaboos University, Muscat, Oman, email: srengaraj1971@gmail.com

Received 20 April 2019; Accepted 3 November 2019

### ABSTRACT

The degradation of levofloxacin by bismuth vanadate (BiVO<sub>4</sub>) catalyst and visible light was carried out in aqueous solution under optimized conditions. The drug degradation was monitored by observing the change in its absorbance value (1290 nm) using a spectrometer. Levofloxacin degraded by almost 76% in 170 min under optimized conditions and followed the first order kinetics (rate constant was 0.0089 min<sup>-1</sup>). LC-MS technique, in addition to tandem mass spectrometry, was used to elucidate the structures of the proposed transformation products/intermediates. Three main initial products were determined after 30 min of reaction (Compound I Fig. 4: (S)-9-fluoro-2,3-dihydro-3-methyl-10-(4-methylpiperazin-1-yl)-[1,4]oxazino-[2,3,4-ij]quinolin-7-one, Compound IV Fig. 4: (S)-3,7-dihydro-3-methyl-10-(4-methylpiperazin-1-yl)-7-oxo-2H-[1,4]oxazino-[2,3,4-ij]quinolone-6-carboxylic acid, and Compound X Fig. 5: (S)-3,7-dihydro-9-hydroxy-3-methyl-7-oxo-10-(piperazine-1-yl)-2H-[1,4]oxazino-[2,3,4-ij]quinolone-6-carboxylic acid). Several pathways for the degradation of levofloxacin can be recognized. They involve mechanisms such as demethylation, defluorination, decarboxylation, deamination, and hydroxylation resulting in the production of many different transformation products such as malonic acid, piperazine, acetaldehyde, pyridone, and methylketone.

**Keywords:** Levofloxacin; Photocatalytic degradation; Transformation products; Mechanism; BiVO<sub>4</sub>; Visible light

### 1. Introduction

Recent trends in environmental science have focused on the removal of pharmaceuticals and their metabolites in water bodies. The presence of pharmaceuticals in the environment can result in exposure to non-target organisms with wide ranging impacts. Extensive use of antibiotics and

antimicrobial products has led to antibiotic resistance in bacteria [1]. Moreover, a variety of aquatic organisms have shown accumulated levels of prescription hormones, antimicrobials, and antidepressants [2]. These drugs, which are up to 90% excreted in its original form, after human consumption, can seep into surface and ground water from domestic wastewater besides some effluents [3,4].

\* Corresponding author.

Photocatalysis is one of the leading advanced oxidation process (AOP) that degrades various organic compounds and has been used extensively for the degradation of pharmaceutical compounds in aqueous solution [5–7]. Recently, various AOPs have been proposed for the degradation of levofloxacin. Among others combined Fenton persulfate [8], heterogeneous photocatalysis [9,10], sonolysis [11] and semiconductor photocatalysis using different metal oxides/sulfides (BiOCl/NaNbO<sub>3</sub> [12], BiMoO<sub>6</sub>/CdS [13], WO<sub>3</sub>/graphene-based metal oxides) [14]. Under the influence of these processes, levofloxacin is eventually converted to smaller moieties which are less harmful to the environment.

Attempt by various researchers have been made to develop various heterogeneous catalysts with increased oxidative power. These mostly include metal and non-metal doped catalysts [15].

Bismuth-based metal oxides such as BiVO<sub>4</sub>, Bi<sub>2</sub>WO<sub>6</sub>, etc. have been reported as novel compounds [16–18], which show enhanced photocatalytic efficiency and improved charge transfer [19–21]. Bismuth vanadate (BiVO<sub>4</sub>) has exceptional properties, including narrow band gap (~2.4 eV), resistance to corrosion, non-toxicity and good dispersibility. It is also stable to visible light in addition to its ability to degrade pollutants [22–25].

Levofloxacin is a widely used second-generation fluoroquinolone antibiotic and as much as 87% of an oral dose was discharged in urine within 2 d [26]. Typical levels of levofloxacin in treated wastewater were found to be in the range of 0.094–0.506 µg/L [27]. Therefore, levofloxacin can be considered as a pollutant which needs to be removed from water bodies.

The objective of this study is to degrade Levofloxacin in the presence of BiVO<sub>4</sub> and visible light under optimized conditions such as pH, drug concentration and catalyst loading. In addition, isolation, characterization, and identification of the transformation products formed during degradation process were detected using LC-MS technique. Plausible degradation pathways and reaction mechanism of the drug degradation were proposed.

## 2. Experimental

Bismuth nitrate pentahydrate (Bi(NO<sub>3</sub>)<sub>3</sub>·5H<sub>2</sub>O), ammonium monovanadate (NH<sub>4</sub>VO<sub>3</sub>), acetic acid (CH<sub>3</sub>COOH), nitric acid (HNO<sub>3</sub>), and levofloxacin (C<sub>18</sub>H<sub>20</sub>FN<sub>3</sub>O<sub>4</sub>) 99% purity were purchased from Sigma-Aldrich. All chemicals were used without further purification. Solutions were prepared in double distilled obtained from a Milli-Q® water purification system.

### 2.1. Catalyst preparation and characterization

BiVO<sub>4</sub> was prepared according to the literature [28–31] by co-precipitation method with bismuth nitrate pentahydrate, and ammonium monovanadate, with a stoichiometric proportion of (1:1, Bi:V). 5 g of (Bi(NO<sub>3</sub>)<sub>3</sub>·5H<sub>2</sub>O) was dissolved in 150 mL 4 M acetic acid, whereas, ammonium monovanadate was dissolved in 300 mL deionized water. The two solutions were mixed and stirred at room temperature. A given amount of concentrated nitric acid was added to adjust the pH to 2. The resulting yellow colloidal solution

was left under constant stirring for 2 d followed by evaporating the excess solvent. Finally, the obtained powder was calcinated at 600°C for 6 h. Under this condition, there is a phase change from tetragonal to monoclinic at 600°C, which is the active phase under visible light. Characterization of the catalyst was done using X-ray diffraction (XRD), energy-dispersive X-ray spectroscopy (EDS), UV-Vis diffuse reflectance spectroscopy (UV-Vis DRS), scanning electron microscope (SEM) and BET. A Shimadzu UV-3600 UV-Vis spectrophotometer (Shimadzu, Japan) was used for UV-Vis DRS measurements using BaSO<sub>4</sub> as a reference standard. XRD was conducted on a Shimadzu-6100 powder XRD diffractometer (40 kV–40 mA), Cu-K<sub>α</sub> radiation, (λ<sub>Kα</sub> = 1.542 Å) with a OneSight new wide-range high-speed detector. Diffractogram was recorded in the range of 2θ = 20°–80° with a rate of 2 deg/min. SEM images and EDS were obtained using JEOL JSM-6010LA (JEOL, Japan). After film preparation on ITO-coated glass, samples were rinsed and allowed to dry. Images and data were then collected at accelerating voltage of 20 kV.

### 2.2. Photocatalytic degradation of levofloxacin

Initially, the degradation of the drug was carried out under different conditions, such as amount of catalyst, pH, and irradiation time. The optimized conditions for maximum drug degradation were as follows: 0.025 g BiVO<sub>4</sub>/100 mL of [Levofloxacin] = 1 × 10<sup>-5</sup> M at pH = 6. The drug solution and the catalyst were allowed to equilibrate, with stirring, for a given time (usually 15–30 min) in the dark before exposure to the light source using a photo-reactor (Luzchem, Canada, 12 visible lamps, cool white light, LZC-420 white phosphore). A sample was then taken from this irradiated mixture at 0, 10, 20, 30, 50, 75, 100, and 170 min. The latter was centrifuged, and the clear solution was transferred to a 1 cm quartz cell for absorbance measurements using a Specord® 210 plus UV/Vis spectrophotometer (Analytik Jena, Germany). The degradation was monitored at λ<sub>max</sub> 290 nm for levofloxacin and the rate constant was then calculated. Power/intensity of visible light was measured to be 11,930 Lux (or 45 mW/cm<sup>2</sup>).

### 2.3. LC-UV/Vis-MS – product analysis and identification

A Waters Acquity UPLC BEH Shield RP 18 column (1.7 µm particle size, 2.1 mm × 150 mm) (Waters, UK) was used for separation of the degradation products on a Shimadzu Nexera-i series LC-2040 liquid chromatograph (Shimadzu, Japan) with quaternary solvent gradient pump and a photodiode array detector. The oven temperature was fixed at 50°C. The diode array detector had a range of wavelengths 200–800 nm and signals were recorded using LabSolution® software. The mobile phase consisted of 85% CH<sub>3</sub>CN and 15% aqueous buffer solution (20 mM NH<sub>4</sub>HCO<sub>2</sub>, pH 4.3). Other conditions were 0.2 mL/min flow rate and 5 µL injection volume. Detection was performed on a triple quadrupole mass spectrometer LC-MS 8030 (Shimadzu, Japan) coupled with an electrospray ionization source and operated in positive polarity with following conditions: interface bias voltage: +4.5 kV, interface bias current = 0.73 µA V; the nebulizer gas flow = 1.5 L min<sup>-1</sup>; drying gas flow = 15 L min<sup>-1</sup>

and drying temperature = 400°C. The mass range was from  $m/z$  50 to 400 Da.

### 3. Results and discussion

#### 3.1. Physical properties of $\text{BiVO}_4$

Characterization of the catalyst was done using XRD, EDS, UV-Vis diffuse reflectance spectroscopy (UV-Vis DRS), SEM and BET. The band gap energies were calculated using the results from the DRS spectra and the application of the Tauc Plot method and is shown in Fig. S1. In this figure,  $h\nu$  is the energy of the light on the abscissa and the quantity  $(\alpha h\nu)^2$  is on the ordinate, where  $\alpha$  is the absorption coefficient of the material. The band gap ( $E_g$ ) was found from this figure to be 2.42 eV.

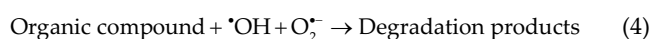
EDS trace of  $\text{BiVO}_4$  photocatalyst is shown in Fig. S2. Bi, V, and O were the only elements which appeared in the EDS trace. XRD and SEM images are presented in Figs. S3 and S4, respectively. All the detectable peaks could be indexed as the monoclinic scheelite bismuth vanadate ( $m\text{-BiVO}_4$ ). The lattice parameter of  $m\text{-BiVO}_4$  is summarized in Table S1. SEM result shows irregular sphere like morphology of prepared  $m\text{-BiVO}_4$ .

#### 3.2. Principles of photocatalysis

A photocatalytic reaction is initiated by the absorption of light by the catalyst followed by the generation of electron ( $e^-$ ) and hole ( $h^+$ ) pairs, which diffuse to the surface (conduction band, CB) where further reaction takes place such as photo-reduction and photo-oxidation. The photogenerated entities react with  $\text{O}_2$  and  $\text{H}_2\text{O}$  to produce  $\text{O}_2^{\bullet-}$  and  $\bullet\text{OH}$  which can decompose organic molecules in solutions. These species are well documented in the literature and their reactions are also well known [32–34]. A summary of these reactions are given below:



where  $e_{\text{cb}}^-$  and  $h_{\text{vb}}^+$  are the electrons in CB and the electron vacancy in VB, respectively.



#### 3.3. Degradation of levofloxacin under optimized conditions

Preliminary experiments were performed with or without visible light or  $\text{BiVO}_4$ . Neither light nor the catalyst by itself degraded levofloxacin molecule (Fig. S5). However, a combination of both visible light and  $\text{BiVO}_4$  caused the degradation of the drug. Levofloxacin exhibits two absorption peaks at 290 and 335 nm. The lower wavelength band is due to  $\pi\text{-}\pi^*$  excitation while the higher wavelength peak is generated due to  $n\text{-}\pi^*$  transition. The two characteristic

absorption peaks decreased significantly, indicating the breakdown of the drug molecule. The 290 nm wavelength was used for further studies in this work. The decrease in absorption intensity of levofloxacin was recorded at fixed times as shown in Fig. 1. Percentage (%) degradation of the drug was calculated as follows:

$$\% \text{ degradation} = \left[ \frac{A_0 - A}{A_0} \right] \times 100 \quad (5)$$

where  $A_0$  = initial absorbance of the drug solution, and  $A$  = absorbance of the drug solution at time  $t$ . It was found that levofloxacin degraded by almost 76% in 170 min under optimized conditions. Levofloxacin degradation fitted best to the pseudo-first-order kinetic equation:

$$\ln \left[ \frac{C}{C_0} \right] = -k_{\text{obs}} t \quad (6)$$

where  $C_0$  = initial concentration of the drug solution, and  $C$  = concentration of the drug solution at time  $t$ ,  $k_{\text{obs}}$  = observed reaction rate constant and was found to be  $0.0089 \text{ min}^{-1}$  with  $R^2 = 0.9882$  as shown in Fig. S6.

#### 3.4. LC/MS studies of levofloxacin degradation

The degradation of any pharmaceutical compound results in the formation of intermediates which are inherently different in their mass number, thus their isolation and characterization require the use of suitable analytical techniques. In this regard, LC-UV/VIS-MS plays an important role. The drug, in the presence of both visible light and the catalyst, showed an appreciable degradation in 170 min. The three dimension chromatograms were monitored at wavelengths range of 200–800 nm. Fig. S7 shows the 3D

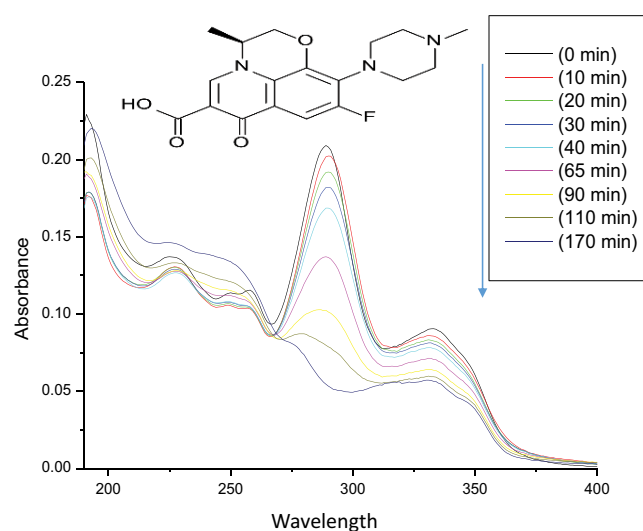


Fig. 1. Change in absorbance spectra of levofloxacin with time. Initial concentration of levofloxacin was  $1 \times 10^{-5} \text{ M}$ , concentration of  $\text{BiVO}_4$  was 0.025 g/100 mL solution, pH 6 and at room temperature.

chromatogram plot for the separation of the drug before and after the treatment. The appearance of new bands in the chromatogram after treatment indicates the formation of new compounds. The masses of the new compounds formed from degradation were analyzed using mass spectrometry. Fig. 2 shows the LC-MS chromatogram of the main products which were formed in the initial stages (30 min). Fig. 3 shows the MS/MS spectra of four intermediate products namely  $m/z$  125, 127, 151, and 211. The identity of these transformation products was confirmed using tandem mass spectrometry and was assigned as structures I, IV, and X as shown in Figs. 4 and 5. Table 1 summarizes the results from MS/MS measurements.

### 3.5. Proposed mechanistic pathways of levofloxacin degradation

When visible light falls on the catalyst ( $\text{BiVO}_4$ ), hydroxyl radicals ( $\cdot\text{OH}$ ) are produced in aqueous medium through a series of reactions involving promotion of electrons from the conduction band to the valence band, water and oxygen molecules [25]. These hydroxyl radicals and super oxide radical anion ( $\text{O}_2^{\cdot-}$ ) are well known to be produced in similar cases and have been reportedly detected using electron spin resonance techniques [6,35]. Hydroxyl radicals ( $\cdot\text{OH}$ ) are very

short lived ( $\sim 70$  ns) and have a diffusion coefficient value of  $\sim 2.3 \times 10^{-5} \text{ cm}^2 \text{ s}^{-1}$ . Thus they will react with any organic molecules within an average range of  $180 \text{ \AA}$  [36].  $\cdot\text{OH}$  radicals react with the drug to form intermediates [6]. LC-MS analysis was used to monitor the intermediates/transformation products. Based on the fragmentation pattern of the compounds in MS/MS studies, chemical structures were proposed and are correlated in Figs. 4 and 5.

Several pathways for the degradation of levofloxacin can be recognized. They involve mechanisms such as demethylation, defluorination, decarboxylation, deamination, and hydroxylation. The general arrow-electron pushing of these processes are amply discussed in our previous publication [37]. All these mechanisms involve reactive  $\cdot\text{OH}$  radicals. These unselective radicals react with the substrate to make new radicals, which are either quenched or enter in a series of other radical reactions, which consequently lead to the degradation products.

The first pathway (Fig. 4) involves the decarboxylation of levofloxacin, mediated by  $\cdot\text{OH}$  radicals, to provide structure I ( $m/z$  317). The unsaturated piperidone is opened and  $\text{O}=\text{C}-\text{CH}=\text{CH}$  unit is lost, probably as malonic acid ( $\text{HO}_2\text{CCH}_2\text{CO}_2\text{H}$ ), to give structure II ( $m/z$  265). Structure III ( $m/z$  317) is formed by the elimination of a piperazine moiety

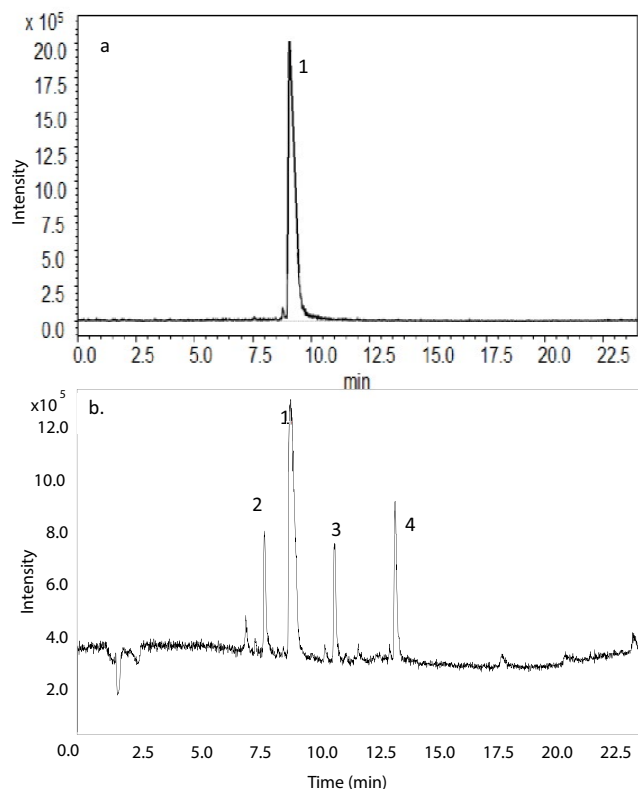


Fig. 2. LC-MS chromatograms of levofloxacin drug (a) before degradation and (b) after 30 min of degradation with  $\text{BiVO}_4$ /visible light. Peaks (1) drug,  $t_R = 9.25$  min,  $m/z$  361, (2) compound IV,  $\text{C}_{18}\text{H}_{21}\text{N}_3\text{O}_4$ ,  $t_R = 7.95$  min,  $m/z$  343, (3) compound X,  $\text{C}_{17}\text{H}_{19}\text{N}_3\text{O}_3$ ,  $t_R = 10.9$  min,  $m/z$  345, (4) compound I,  $\text{C}_{17}\text{H}_{20}\text{NF}_3\text{O}_2$ ,  $t_R = 13.6$  min,  $m/z$  317. Initial concentration of levofloxacin was  $1 \times 10^{-5} \text{ M}$ , concentration of  $\text{BiVO}_4$  was  $0.025 \text{ g/100 mL}$  solution, pH 6 and at room temperature.

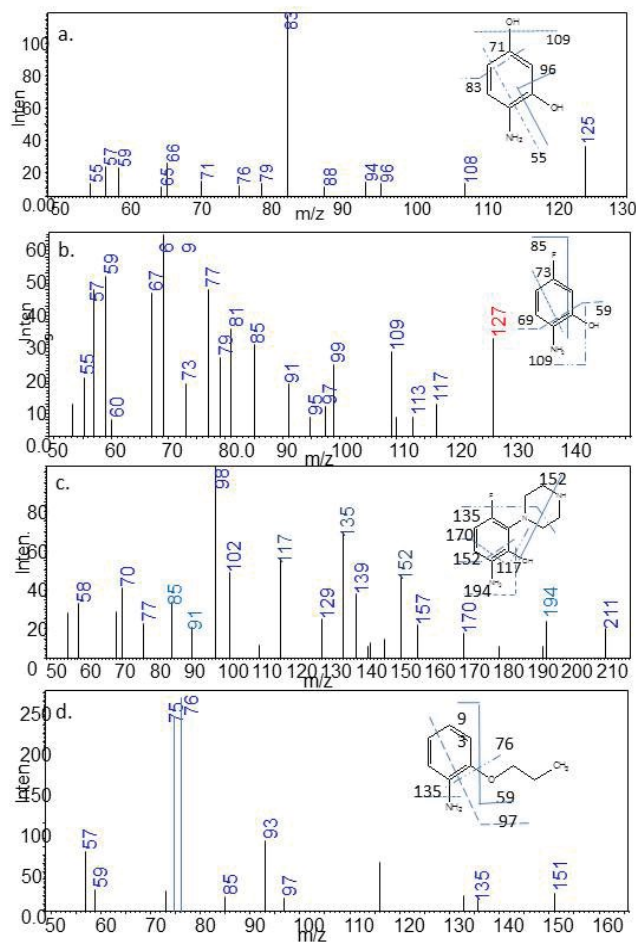


Fig. 3. Tandem mass spectra of four transformation products of levofloxacin.

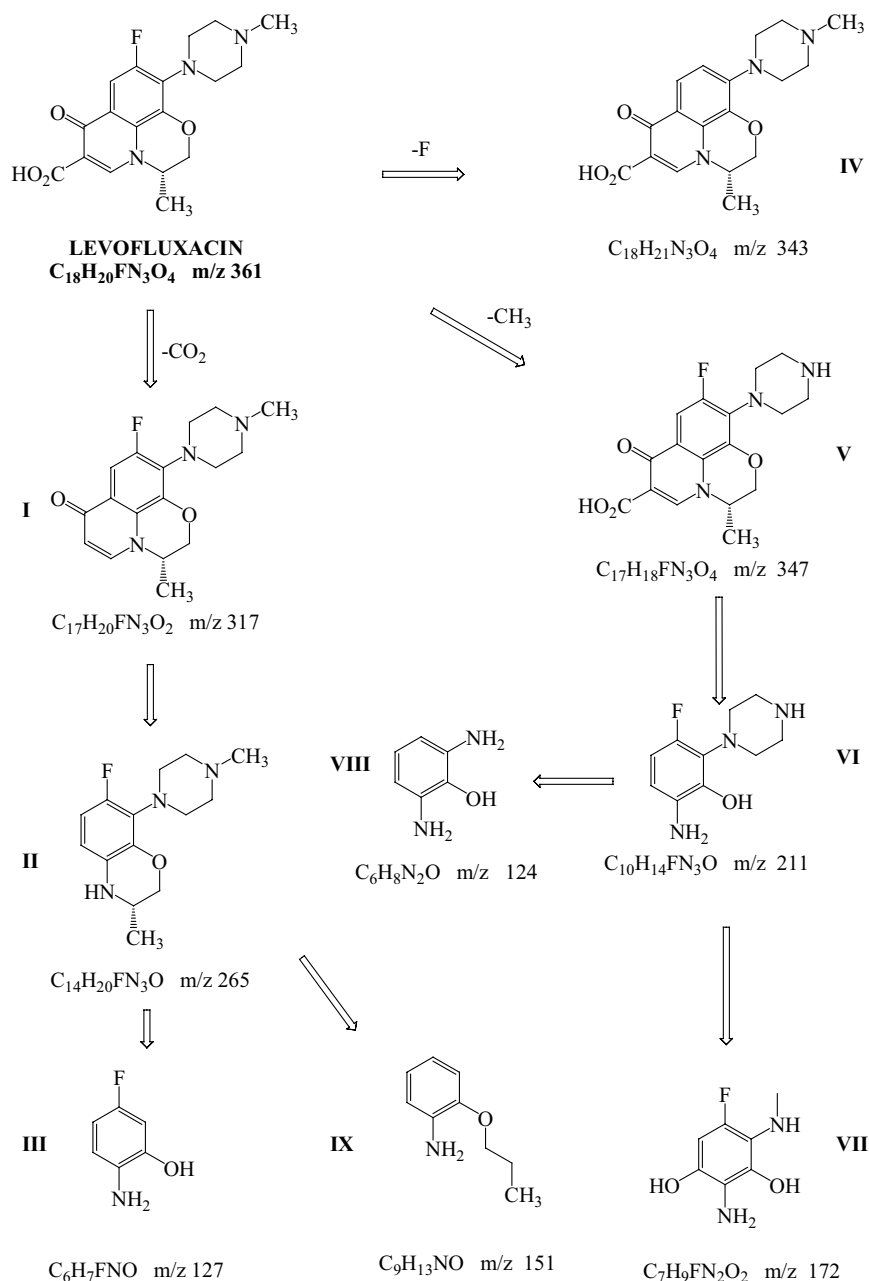


Fig. 4. Pathway involving demethylation and defluorination of levofloxacin.

and ring opening of the morpholine structure with loss of a  $CH_2CH(CH_3)$  unit. Levofloxacin can also be defluorinated to structure IV ( $m/z$  343). Another observed degradation route involves the demethylation of levofloxacin to give structure V ( $m/z$  347). This compound underwent loss of small units to yield structure VI ( $m/z$  211). The latter was converted to structure VII ( $m/z$  172) by the loss of most of the piperazine carbon skeleton and subsequent hydroxylation. Compound VI can also be defluorinated and the piperazine converted primary amine VIII ( $m/z$  124). Structure II also gave rise to compound IX ( $m/z$  151).

An alternative degradation sequence identified in this study (Fig. 5) is the defluorination and hydroxylation of

demethylated levofloxacin compound V to generate structure X ( $m/z$  345). The latter is further hydroxylated to structure XI ( $m/z$  375). Hydroxylation of X led to compound XIII ( $m/z$  361). Compound XIV ( $m/z$  125) can be traced back to structure X after major loss of structural units. The pyridone unit V gives rise to methyl ketone XII ( $m/z$  209). We propose mechanisms for the degradation of pyridone I  $\rightarrow$  II and morpholine II  $\rightarrow$  III, which to our knowledge, has not been reported in the literature.

An  $\cdot OH$  conjugate addition to the unsaturated pyridone gives an  $\alpha$ -carbon radical (Fig. 6, structure 1) which in turn forms a ketene 2, which is hydrolyzed to an acid. The ensuing phenyl radical is quenched with an  $H\cdot$  to yield

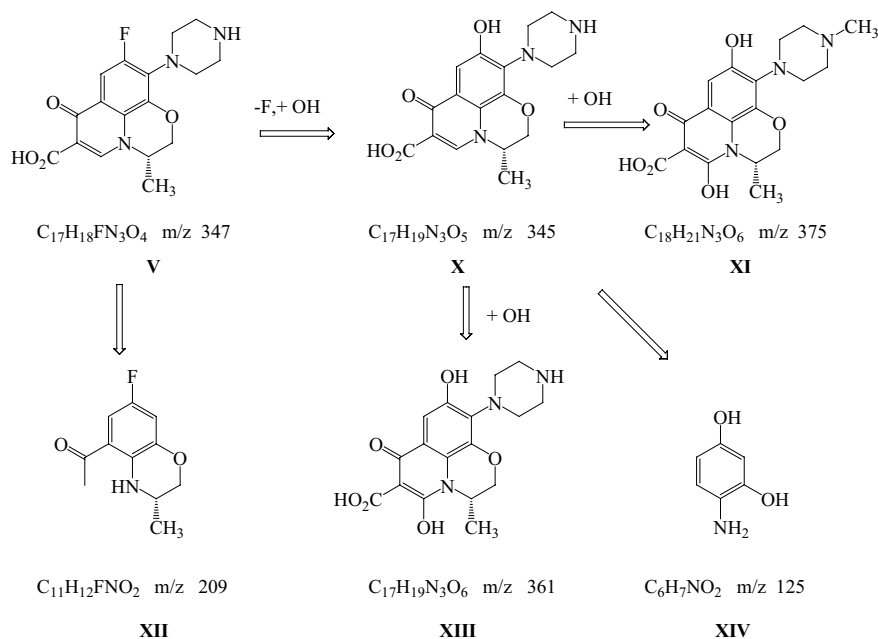


Fig. 5. Pathway involving hydroxylation of degraded levofloxacin.

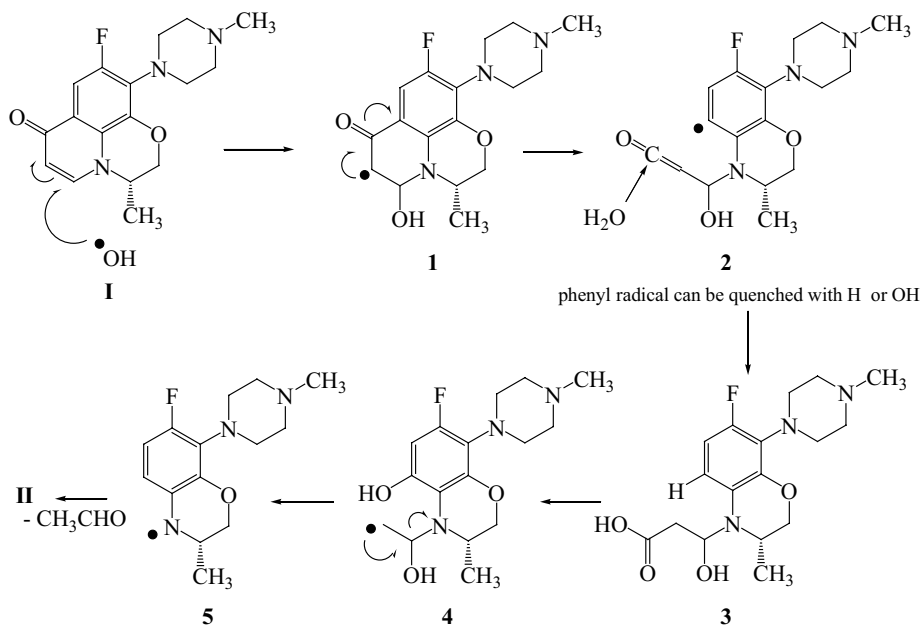


Fig. 6. Proposed mechanism for degradation of pyridone ring (I  $\rightarrow$  II).

structure 3. It should be noted that the hydroxylated compound VII (Fig. 4) could result from a similar phenyl radical quenching by  $\cdot OH$ . Decarboxylation of 3 followed by cleavage of the resulting radical 4 yields acetaldehyde and an amine radical 5. The latter forms amine II.

The conversion of the morpholine structure II (Fig. 7) occurs through a nitrogen radical cation 6 followed by the cleavage of a C–N bond to produce secondary radical 7. Structure 7 forms propene and a stable phenolic radical which is then converted to III.

A close analysis of the proposed pathways suggests that the initial degradation occurs through one of the following mechanisms namely, decarboxylation, demethylation and defluorination. The order of these operations cannot be ascertained and are most probably occurring simultaneously. Comparison of our work with the literature finding reveals a completely different set of degradation products using  $Bi_2WO_6$  photocatalyst/visible light [6]. Their suggested mechanism is dissimilar from the one we are suggesting.

Table 1  
MS-MS data of various intermediates formed from levofloxacin degradation

Precursor ion mass	Product ion masses
124	108, 96, 83, 70, 55
125	109, 96, 83, 71, 55
127	109, 83, 73, 69, 59, 57
151	135, 97, 93, 76, 59
172	154, 136, 125, 101, 90, 73
209	194, 166, 151, 137, 93, 74
211	194, 170, 152, 35, 117
265	219, 113, 102
343	325, 240, 171, 147, 102,
345	330, 316, 301, 288, 216, 173
347	303, 288, 262, 248, 230, 218, 186
361	343, 317, 302, 287, 274, 246
375	357, 331, 315, 290, 275, 214, 174

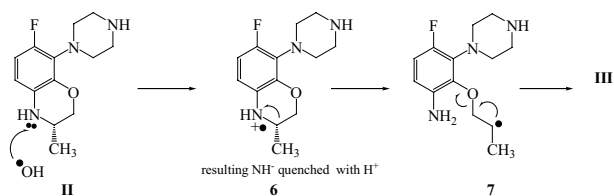


Fig. 7. Proposed mechanism for degradation of morpholine ring (II → III).

#### 4. Conclusion

$\text{BiVO}_4$  was prepared and characterized; then it was used with visible light to degrade levofloxacin which showed 76% degradation in 170 min. The reaction followed pseudo-first-order kinetics. The LC-MS and MS/MS methods were used to separate and identify the transformation products. The preliminary products after 30 min of reaction were of  $m/z$  values of 317 (compound I), 345 (compound IV) and 343 (compound X). Several mechanisms for the degradation of levofloxacin were observed including demethylation, defluorination, decarboxylation, deamination, and hydroxylation. Many low molecular weight final products were detected such as malonic acid, piperazine, acetaldehyde, pyridone, and methylketone.

#### Acknowledgment

The authors would like to thank the United Arab Emirates University for providing the financial support through fund numbers (31S218), (31S281) and (31R046).

#### References

- [1] S.B. Zaman, M.A. Hussain, R. Nye, V. Mehta, K.T. Mamun, N. Hossain, A Review on antibiotic resistance: alarm bells are ringing, *Cureus*, 9 (2017) 1403–1412.
- [2] M.I. Farré, S. Pérez, L. Kantiani, D. Barceló, Fate and toxicity of emerging pollutants, their metabolites and transformation products in the aquatic environment, *TrAC Trends Anal. Chem.*, 27 (2008) 991–1007.
- [3] C.G. Daughton, *Pharmaceutical Ingredients in Drinking Water: Overview of Occurrence and Significance of Human Exposure*, in: *Contaminants of Emerging Concern in the Environment: Ecological and Human Health Considerations*, American Chemical Society, 2010, pp. 9–68.
- [4] R.T. Williams, *Human Pharmaceuticals: Assessing the Impacts on Aquatic Ecosystems*, in: SETAC Press, Pensacola, FL, 2005.
- [5] A.S. Giri, A.K. Golder, Ciprofloxacin degradation in photo-Fenton and photo-catalytic processes: degradation mechanisms and iron chelation, *J. Environ. Sci.*, 80 (2019) 82–92.
- [6] A. Kaur, S.K. Kansal,  $\text{Bi}_2\text{WO}_6$  nanocuboids: an efficient visible light active photocatalyst for the degradation of levofloxacin drug in aqueous phase, *Chem. Eng. J.*, 302 (2016) 194–203.
- [7] J. Trawinski, R. Skibinski, Photolytic and photocatalytic degradation of the antipsychotic agent tiapride: kinetics, transformation pathways and computational toxicity assessment, *J. Hazard. Mater.*, 321 (2017) 841–858.
- [8] I. Epold, M. Trapido, N. Dulova, Degradation of levofloxacin in aqueous solutions by Fenton, ferrous ion-activated persulfate and combined Fenton/persulfate systems, *Chem. Eng. J.*, 279 (2015) 452–462.
- [9] S.K. Kansal, P. Kundu, S. Sood, R. Lamba, A. Umar, S.K. Mehta, Photocatalytic degradation of the antibiotic levofloxacin using highly crystalline  $\text{TiO}_2$  nanoparticles, *New J. Chem.*, 38 (2014) 3220–3226.
- [10] S. Sharma, A. Umar, S.K. Mehta, A.O. Ibadon, S.K. Kansal, Solar light driven photocatalytic degradation of levofloxacin using  $\text{TiO}_2$ /carbon-dot nanocomposites, *New J. Chem.*, 42 (2018) 7445–7456.
- [11] W. Guo, Y. Shi, H. Wang, H. Yang, G. Zhang, Sonochemical decomposition of levofloxacin in aqueous solution, *Water Environ. Res.*, 82 (2010) 696–700.
- [12] J. Xu, B. Feng, Y. Wang, Y. Qi, J. Niu, M. Chen,  $\text{BiOCl}$  decorated  $\text{NaNbO}_3$  nanocubes: a novel p-n heterojunction photocatalyst with improved activity for ofloxacin degradation, *Front. Chem.*, 6 (2018) 9p, <https://doi.org/10.3389/fchem.2018.00393>.
- [13] S. Li, Y. Liu, Y. Long, L. Mo, H. Zhang, J. Liu, Facile synthesis of  $\text{Bi}_2\text{MoO}_6$  microspheres decorated by CdS nanoparticles with efficient photocatalytic removal of levofloxacin antibiotic, *Catalysts*, 8 (2018) 477.
- [14] M.Y. Khan, M. Ahmad, S. Sadaf, S. Iqbal, F. Nawaz, J. Iqbal, Visible light active indigo dye/graphene/ $\text{WO}_3$  nanocomposites with excellent photocatalytic activity, *J. Mater. Res. Technol.*, 8 (2019) 3261–3269.
- [15] Z. Qiao, T. Yan, W. Li, B. Huang, In situ anion exchange synthesis of  $\text{In}_2\text{S}_3/\text{In}(\text{OH})_3$  heterostructures for efficient photocatalytic degradation of MO under solar light, *New J. Chem.*, 41 (2017) 3134–3142.
- [16] J. Romão, D. Barata, N. Ribeiro, P. Habibovic, H. Fernandes, G. Mul, High throughput screening of photocatalytic conversion of pharmaceutical contaminants in water, *Environ. Pollut.*, 220 (2017) 1199–1207.
- [17] M. Sayed, L.A. Shah, J.A. Khan, N.S. Shah, J. Nisar, H.M. Khan, P. Zhang, A.R. Khan, Efficient photocatalytic degradation of norfloxacin in aqueous media by hydrothermally synthesized immobilized  $\text{TiO}_2/\text{Ti}$  films with exposed {001} facets, *J. Phys. Chem. A*, 120 (2016) 9916–9931.
- [18] I. Corsi, M. Winther-Nielsen, R. Sethi, C. Punta, C. Della Torre, G. Libralato, G. Lofrano, L. Sabatini, M. Aiello, L. Fiordi, F. Cinuzzi, A. Caneschi, D. Pellegrini, I. Buttino, Ecofriendly nanotechnologies and nanomaterials for environmental applications: key issue and consensus recommendations for sustainable and ecosafe nanoremediation, *Ecotoxicol. Environ. Saf.*, 154 (2018) 237–244.
- [19] H. Huang, L. Liu, Y. Zhang, N. Tian, Novel  $\text{BiIO}_4/\text{BiVO}_4$  composite photocatalyst with highly improved visible-light-induced photocatalytic performance for rhodamine B degradation and photocurrent generation, *RSC Adv.*, 5 (2015) 1161–1167.
- [20] L. Chen, D. Meng, X. Wu, A. Wang, J. Wang, M. Yu, Y. Liang, Enhanced visible light photocatalytic performances

- of self-assembled hierarchically structured  $\text{BiVO}_4/\text{Bi}_2\text{WO}_6$  heterojunction composites with different morphologies, *RSC Adv.*, 6 (2016) 52300–52309.
- [21] M. Palmi, E.M. Zahran, S. Angarano, S. Balint, Z. Paszti, M.R. Knecht, L.G. Bachas, Pd-decorated  $\text{m-BiVO}_4/\text{BiOBr}$  ternary composite with dual heterojunction for enhanced photocatalytic activity, *J. Mater. Chem. A*, 5 (2017) 529–534.
- [22] Y. Hu, J. Fan, C. Pu, H. Li, E. Liu, X. Hu, Facile synthesis of double cone-shaped  $\text{Ag}_3\text{V}_2\text{O}_7/\text{BiVO}_4$  nanocomposites with enhanced visible light photocatalytic activity for environmental purification, *J. Photochem. Photobiol. A*, 337 (2017) 172–183.
- [23] D. Lv, D. Zhang, X. Pu, D. Kong, Z. Lu, X. Shao, H. Ma, J. Dou, One-pot combustion synthesis of  $\text{BiVO}_4/\text{BiOCl}$  composites with enhanced visible-light photocatalytic properties, *Sep. Purif. Technol.*, 174 (2017) 97–103.
- [24] M. Guo, Y. Wang, Q. He, W. Wang, W. Wang, Z. Fu, H. Wang, Enhanced photocatalytic activity of S-doped  $\text{BiVO}_4$  photocatalysts, *RSC Adv.*, 5 (2015) 58633–58639.
- [25] A. Malathi, J. Madhavan, A. Muthupandian, A. Prabhakarn, A review on  $\text{BiVO}_4$  photocatalyst: activity enhancement methods for solar photocatalytic applications, *Appl. Catal. A*, 555 (2018) 47–74.
- [26] G.G. Zhanel, S. Fontaine, H. Adam, K. Schurek, M. Mayer, A.M. Noreddin, A.S. Gin, E. Rubinstein, D.J. Hoban, A Review of new fluoroquinolones: focus on their use in respiratory tract infections, *Treat Respir. Med.*, 5 (2006) 437–465.
- [27] X.-S. Miao, F. Bishay, M. Chen, C.D. Metcalfe, Occurrence of antimicrobials in the final effluents of wastewater treatment plants in Canada, *Environ. Sci. Technol.*, 38 (2004) 3533–3541.
- [28] X. Zhang, Z. Ai, F. Jia, L. Zhang, X. Fan, Z. Zou, Selective synthesis and visible-light photocatalytic activities of  $\text{BiVO}_4$  with different crystalline phases, *Mater. Chem. Phys.*, 103 (2007) 162–167.
- [29] L. Zhou, W. Wang, S. Liu, L. Zhang, H. Xu, W. Zhu, A sonochemical route to visible-light-driven high-activity  $\text{BiVO}_4$  photocatalyst, *J. Mol. Catal. A*, 252 (2006) 120–124.
- [30] A. Zhang, J. Zhang, N. Cui, X. Tie, Y. An, L. Li, Effects of pH on hydrothermal synthesis and characterization of visible-light-driven  $\text{BiVO}_4$  photocatalyst, *J. Mol. Catal. A*, 304 (2009) 28–32.
- [31] X. Meng, L. Zhang, H. Dai, Z. Zhao, R. Zhang, Y. Liu, Surfactant-assisted hydrothermal fabrication and visible-light-driven photocatalytic degradation of methylene blue over multiple morphological  $\text{BiVO}_4$  single-crystallites, *Mater. Chem. Phys.*, 125 (2011) 59–65.
- [32] H. Huang, S. Tu, C. Zeng, T. Zhang, A.H. Reshak, Y. Zhang, Macroscopic polarization enhancement promoting photo- and piezoelectric-induced charge separation and molecular oxygen activation, *Angew. Chem. Int. Ed.*, 56 (2017) 11860–11864.
- [33] H. Huang, Y. He, X. Li, M. Li, C. Zeng, F. Dong, X. Du, T. Zhang, Y. Zhang,  $\text{Bi}_2\text{O}_2(\text{OH})(\text{NO}_3)$  as a desirable  $[\text{Bi}_2\text{O}_2]^{2+}$  layered photocatalyst: strong intrinsic polarity, rational band structure and {001} active facets co-beneficial for robust photooxidation capability, *J. Mater. Chem. A*, 3 (2015) 24547–24556.
- [34] H. Huang, X. Li, J. Wang, F. Dong, P.K. Chu, T. Zhang, Y. Zhang, Anionic group self-doping as a promising strategy: band-gap engineering and multi-functional applications of high-performance  $\text{CO}_3^{2-}$ -doped  $\text{Bi}_2\text{O}_2\text{CO}_3$ , *ACS Catal.*, 5 (2015) 4094–4103.
- [35] G. Lu, Z. Lun, H. Liang, H. Wang, Z. Li, W. Ma, In situ fabrication of  $\text{BiVO}_4\text{-CeVO}_4$  heterojunction for excellent visible light photocatalytic degradation of levofloxacin, *J. Alloy Compd.*, 772 (2019) 122–131.
- [36] J.W.T. Spinks, R.J. Woods, *An Introduction to Radiation Chemistry*, John Wiley and Sons Inc, USA, 1990.
- [37] S. Hisaindee, M.A. Meetani, M.A. Rauf, Application of LC-MS to the analysis of advanced oxidation process (AOP) degradation of dye products and reaction mechanisms, *TrAC Trends Anal. Chem.*, 49 (2013) 31–44.

### Supplementary information:

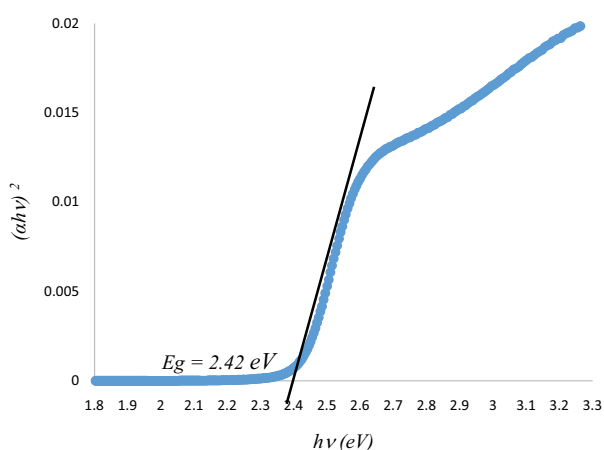


Fig. S1. Tauc plot of  $\text{BiVO}_4$ .

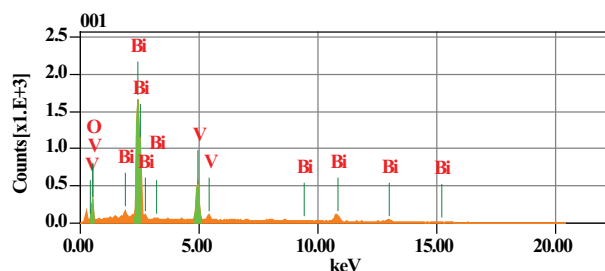


Fig. S2. EDS trace of  $\text{BiVO}_4$ .

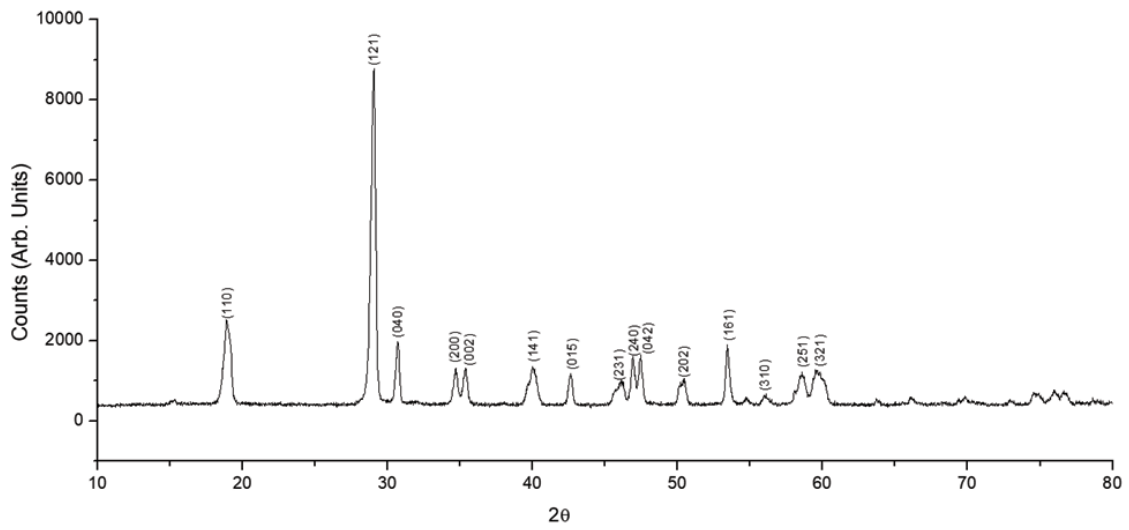


Fig. S3. XRD pattern of  $\text{BiVO}_4$ .

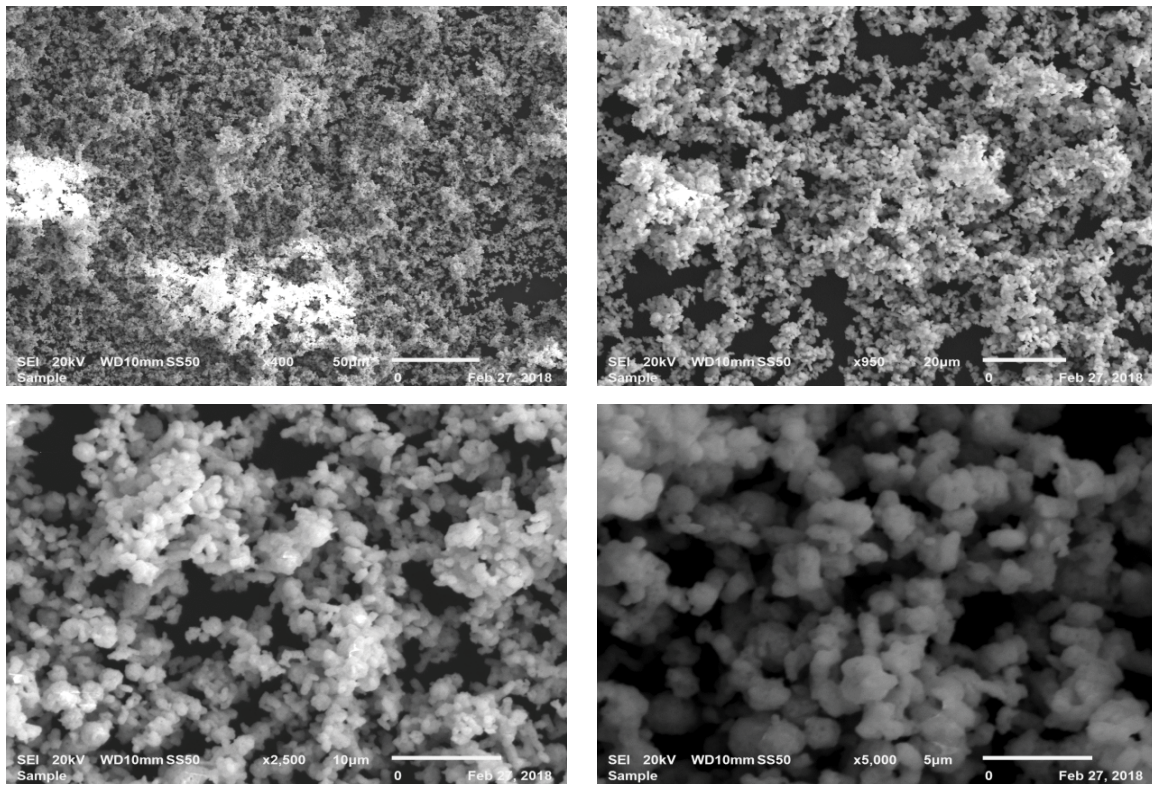


Fig. S4. SEM of  $\text{BiVO}_4$ .

Table S1  
Physical structure parameters of  $\text{BiVO}_4$

Band gap energy (eV)	$S_{\text{BETs}}$ ( $\text{m}^2 \text{g}^{-1}$ )	Pore size (nm)	$V_{\text{pores}}$ ( $\text{cm}^3 \text{g}^{-1}$ )	Lattice constant ( $\text{Å}$ )			Average Crystalline size (nm)	EDS (Atom %)		
				<i>a</i>	<i>b</i>	<i>c</i>		Bi	V	O
2.42	0.9956	5.314	0.00132	5.1702	11.64	5.0738	6.7	32.42	28.96	38.62

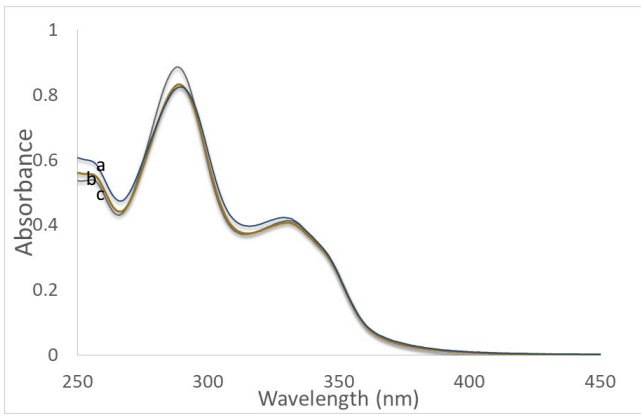


Fig. S5. Absorption spectra of levofloxacin drug: (a) without light and catalyst, (b) with catalyst and no light, (c) with light and no catalyst.

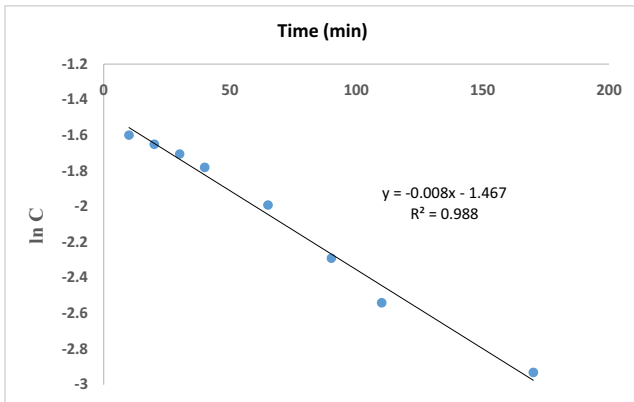


Fig. S6. First order kinetic plot of levofloxacin degradation.

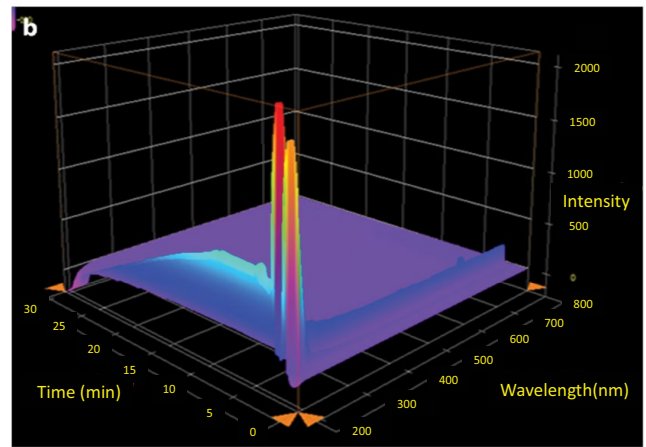
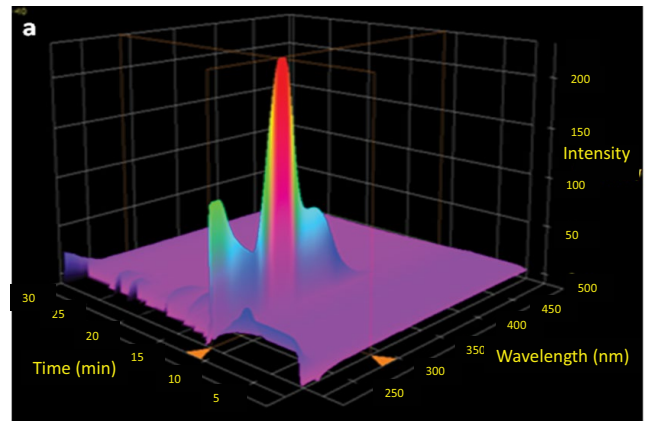


Fig. S7. 3D chromatogram plot of levofloxacin drug: (a) before and (b) after photocatalytic degradation. Initial concentration of levofloxacin was  $1 \times 10^{-5}$  M, concentration of  $\text{BiVO}_4$  was 0.025 g/100 mL solution, pH 6 and at room temperature.